Photoelastic Analysis of Crack Tip Shielding after an Overload

C. Colombo[1], E.A. Patterson[2] and L. Vergani[1]

[1] Dipartimento di Meccanica, Politecnico di Milano, Via La Masa 34, 20156 Milano, ITALY; e-mail: chiara.colombo@mecc.polimi.it; laura.vergani@polimi.it
[2] Department of Mechanical Engineering, Michigan State University, 2555 Engineering Building, East Lansing, MI 48824, USA; e-mail: eann@egr.msu.edu

ABSTRACT. *A quantitative analysis of the interaction fatigue crack propagation and of the shielding effects associated with the plasticity along the flanks and at the tip of a crack has been performed. In two CT polycarbonate specimens, fatigue cracks were grown under low frequency loading: the first followed a nominal cycling, while an overload was applied to the second one and the shielding level monitored. Images of the two tests were collected by means of digital phase-stepping photoelasticity, and isochromatic fringe patterns of the cracks were obtained by a recently developed unwrapping technique. Stress intensity factors were evaluated fitting a mathematical model to isochromatic fringe data. The model separates the effects of applied load and of shielding due to the plasticity at the crack tip and flanks on the propagation and thus allows some qualitative observations to be made on the underlying fatigue mechanisms.*

INTRODUCTION

Crack propagation in components and structures subjected to cyclic fatigue load often involves random or variable amplitude, rather than constant amplitude loading conditions. A change in the loading condition causes significant accelerations and/or retardations to the crack growth. To better assess and predict the fatigue life of these parts, an evaluation of load interaction effects is required. A number of different mechanisms have been proposed to explain the retardation in crack growth observed as the result of even a single overload, but the precise mechanism responsible for this behaviour is not yet fully understood. Experiments provide evidence that after an overload, a region of residual plastic deformation and compressive stresses is created in front of the crack tip, so that the load required crack propagation increases.

This phenomenon is a form of crack closure and was first defined by [1]. Since the discovery of plasticity-induced fatigue crack closure, several other closure mechanisms have been identified. It has been recently recognized that crack closure is better described in terms of crack tip shielding mechanisms. The net effect of the plasticity ahead of the crack tip and along the flanks is to shield the crack tip from some part of the applied stress field.

The mathematical model proposed by [2] aims to separate the contributions of the forces inducing propagation and from those providing shielding. This model takes into account the different forces acting in the crack tip region and along the crack flanks, considering the effect of both applied load and induced plasticity. In particular, it is possible to evaluate the global stress intensity factor K_I decomposed in two different terms: K_F (forward) acting to make the crack propagate and K_R (retardation) representing the retarding stress field parallel to the crack. A further term is introduced, K_S (shear), to characterize the interfacial shear stress at the elastic-plastic boundary in the crack wake. T-stress is also included in the model.

In this paper, a quantitative evaluation of propagating fatigue cracks is presented using photoelasticity, focusing attention on the effect of crack shielding on the propagation. In particular, an overload is applied to one of the observed cracks, and its influence on the fringe pattern is analyzed and directly compared to the case without overload.

EXPERIMENTAL TESTS

Two tests were performed on CT polycarbonate specimens, cut from extruded sheets of 2 mm thickness; the dimensions are as in [3]. Residual stresses in the specimens were removed by a controlled thermal cycle, proposed in [4]. A fatigue crack was grown from the notch of each specimen using a screw-driven testing machine by applying a cyclic load from 10 to 160 N at 0.5 Hz. The choice of this low frequency is directly related to the use of polycarbonate, a visco-elastic material for which higher frequencies can limit the development of the plasticity at the crack tip and along crack flanks. The specimen and the loading frame were surrounded by a polariscope. A camera was placed to collect images during the loading and unloading cycles; images were centred on the crack tip.

In the first specimen, the fatigue crack was grown until the crack propagated in an unstable condition and the specimen exhibited collapse. In Fig. 1.a the crack growth rate of specimen 1 is shown as function of the number of cycles. After an initial linear slope, i.e. a constant growth rate for the crack, , the rate changed at a crack length of 30mm and the crack length increased more rapidly. Thus, it is possible to identify stage of unstable propagation of the fatigue crack in this first tested specimen. This behaviour was observed also in the second specimen (Fig. 1.b). In this specimen, the crack was grown till a length of 27.9 mm and then an overload of 190 N (18.75% of the nominal load) was applied. Crack length increased from 27.9 to 28.6 mm during this single cycle. As a consequence, the propagation rate decreased substantially, thus providing a net beneficial effect from the overload. At around 110 cycles after the overload, the crack was more than 30 mm long and the propagation became unstable.

At the longest crack lengths when unstable propagation occurred, the specimens stiffness decreased and an out-of-plane twisting was observed during testing. For this reason, images collected in these last stages of the test were not processed and no data was consider from either specimen.

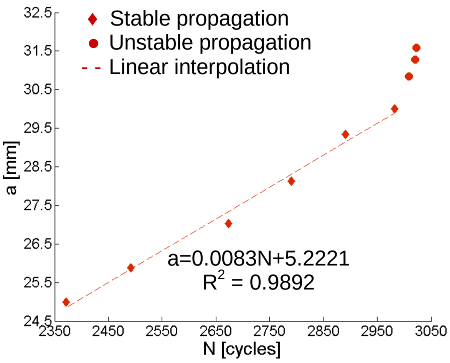

a.

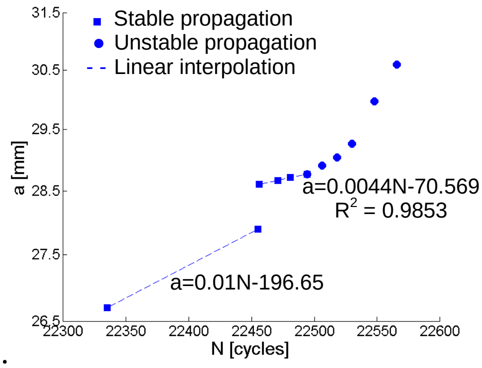

b.

Figure 1: Fatigue growth curves for specimens 1 (a.) and 2 (b.).

Photoelastic Images

Images of the fatigue cracks were collected from the experimental tests, using the algorithm proposed by [5]: a set of 6 images was collected for each step of analysed load and crack length. The first image of this set corresponds to a circular polariscope in a dark field arrangement. In Fig. 2 the fringe pattern obtained for specimen 1 viewed using this arrangement is shown for approximately 1mm increments of crack growth. This set of images was collected at zero load; therefore the fringes are due only to the plastic field in wake and around the crack tip. The fringe orders and the plastic wake size increase with crack length; moreover, when the crack is relatively small, the fringes are closed loops 'attached' to the crack tip, while, with increasing the levels of plasticity, the lower order fringes become open loops and no longer return to the tip.

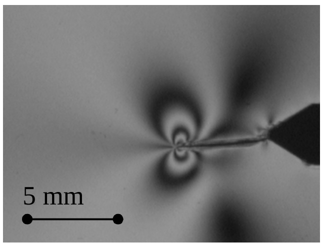

(a) a = 25 mm, N = 2371 cycles

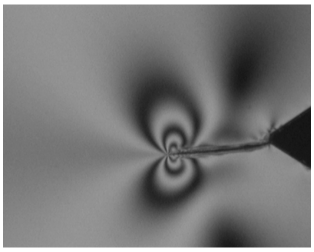

(b) a = 25.87 mm, N = 2492 cycles

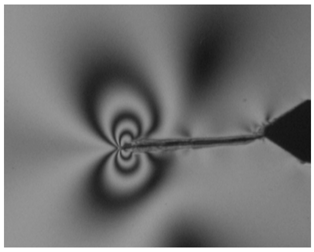

(c) a = 27 mm, N = 2673 cycles

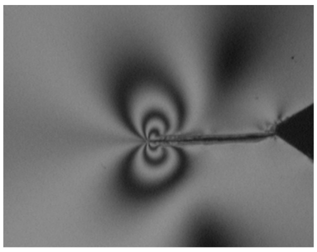

(d) a = 28.13 mm, N = 2790 cycles

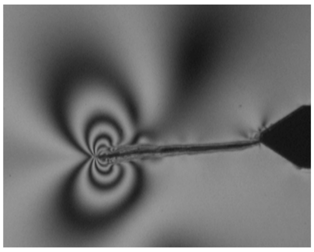

(e) a = 29.34 mm, N = 2891 cycles

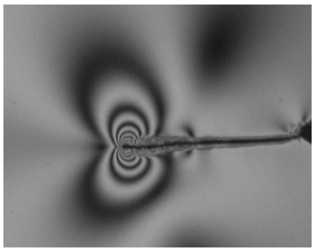

(f) a = 30 mm, N = 2982 cycles

Figure 2: Isochromatic fringe patterns from a dark field circular polariscope for specimen 1 at zero applied load.

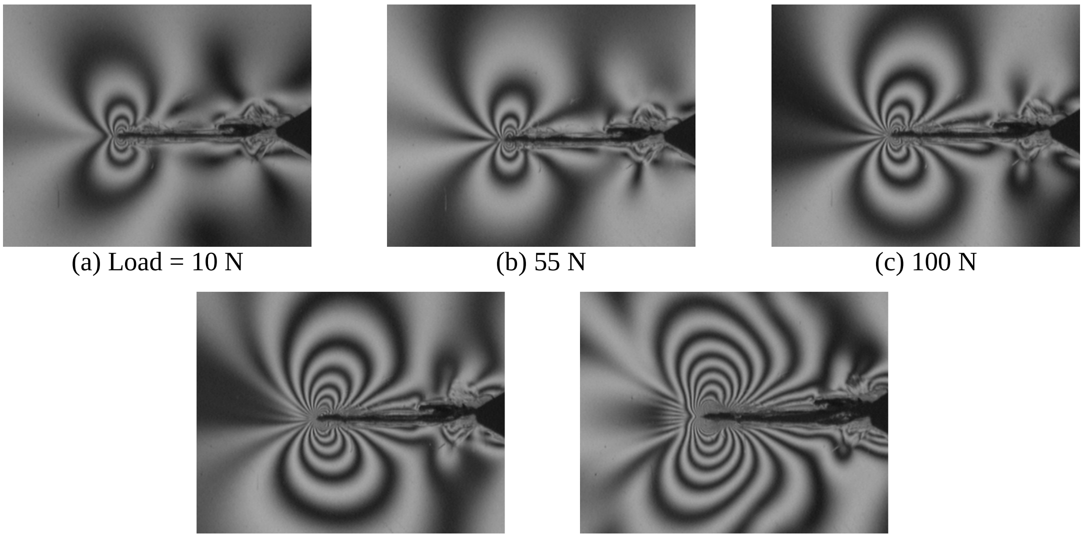

(a) Load = 10 N (b) 55 N (c) 100 N

(d) 145 N (e) 190 N

Figure 3: Isochromatic fringe patterns from a dark field circular Polariscope for specimen 2 during the overload cycle.

At the beginning of the test on specimen 2, two cracks propagated from the notch as shown in Fig. 3, but one of them stopped, so that the test required more cycles to develop a crack of the same length as in specimen 1. At 28 mm crack length, the fringe pattern was similar to that in specimen 1 for the same crack length and the overload was applied. Isochromatic fringe patterns observed during the application of the overload are shown in Fig. 3. These fringes increased in order and changed in shape, revealing an increment in the extent plastic deformation. The fringe patterns are significantly more complicated and very dense at the crack tip, where the stress gradient is the highest. After the overload application and the creation of a larger plastic area, the residual fringe pattern at zero load has changed significantly as shown in Fig. 4. Before the overload, there are two distinct set of fringe loops on either side of the crack tip, whereas after the overload the two sets of fringes have merged and have an elliptical shape. Once the crack had propagated through the plastic area created by the overload, the fringe pattern became similar to the original, pre-event shape.

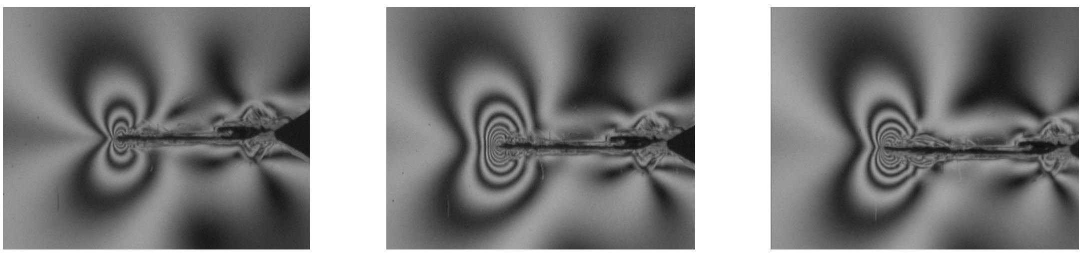

(a) Before the overload (b) End of the overload (c) 110 cycles after the overload

Figure 4: Variation in isochromatic fringe pattern at zero load for specimen 2 before, immediately after and significantly after the overload event.

STRESS FIELD MODEL

Isochromatic fringe data from both specimens are automatically obtained using the unwrapping algorithm proposed by [6] and then the mathematical model proposed in [2], based on the Muskhelishvili's approach was fitted to this data. The model is in the form given below:

$$\frac{Nf}{h} = \left|\sigma_y - \sigma_x + 2i\sigma_{xy}\right| = \left|Az^{-1/2} + Bz^{-1/2}\bar{z} + Cz^0 + Dz^{-1/2}\ln z + Ez^{-3/2}\bar{z}\ln z\right| \tag{1}$$

where:

- N is the fringe order;
- f = 0.007 [MPa·m/fringe] is the material fringe constant;
- h = 0.002 [m] is the specimen thickness;
- x, y are the Cartesian coordinates, with an origin at the crack tip and $z = x + i\,y$;
- $A,\ldots E$ are coefficients that are evaluated by fitting the mathematical model to the experimental data.

In [2] the evaluation of the fracture mechanics parameters is proposed from the constant terms $A,\ldots E$ introduced in Eq.1; assuming E=-D to give the appropriate asymptotic trend along the crack flank, such that:

$$T = -C\,;\quad K_F = \lim_{r\to 0}\left[\sqrt{2\pi r}\left(\sigma_y + 2Er^{-1/2}\ln r\right)\right] = \sqrt{\frac{\pi}{2}}\left(A - 3B - 8E\right);$$
$$K_S = \lim_{r\to 0}\left[\sqrt{2\pi r}\,\sigma_{xy}\right] = \pm\sqrt{\frac{\pi}{2}}\left(A + B\right);\quad K_R = \lim_{r\to 0}\left[\sqrt{2\pi r}\,\sigma_x\right] = \frac{\pi^{3/2}}{\sqrt{2}}\left(D - 3E\right) \tag{2}$$

where:

- T is the T-stress;
- K_F is the stress intensity factor which characterises the stresses tending to propagate the crack and in absence of shielding, E=0 and K_F is equivalent to K_I from the classical definition (in [2] K_F was proposed as K_I);
- K_S is the stress intensity factor which characterises the shear stress at the elastic-plastic boundary at crack flanks; K_S is considered as positive for the top flank (y>0) and negative for the bottom flank (y<0);
- K_R is the retardation intensity factor which characterises the stress shielding the crack propagation, and which arise due to the plasticity at the crack tip;
- r is the distance of the selected pixel from the crack tip.

To obtain A,...E coefficients and estimate the stress intensity factors and the T-stress, an error function was defined as the sum of the least squared differences between the experimental data and the fitted model at all data points. The solution is found as the minimum of this error function and confidence limits were similarly calculated following the methodology in [7].

DATA FROM OVELOAD CYCLE

The results for fracture mechanics parameters are shown in Fig. 5 for a cycle that represents the constant amplitude loading case and the overload cycle. In both cases the crack lengths were nominally the same. The peak values of K_F and K_R are considerably larger in the overload case, as would be expected, however it is interested to note that there signs are inverted at the end of the overload cycle. The latter feature is probably a result of the large plastic field formed ahead of the crack tip. K_S is very small in the constant amplitude case and show no real trends with load but is an order of magnitude greater during the overload and changes direction with unloading. There is little difference in the T-stress values during the loading sections of the cycles but the T-stress collapses dramatically just before the peak load and during the unloading after the overload.

These new fracture parameters clearly reveal additional information about the interaction of plastic zones with the surrounding elastic stress fields during fatigue crack propagation; however further data is needed to allow detailed interpretations to be made.

CONCLUSIONS

In this study experimental fatigue tests on polycarbonate specimens were performed. In conclusion, from the photoelastic data collected and processed using phase-stepping techniques, it was possible to:

- observe the trends in the behaviour of isochromatic fringes in the region of the crack tip, avoiding the influence of the isoclinics;
- fit a mathematical model to the experimental data and obtain fracture mechanics parameters in terms of stress intensity factors interpreting crack propagation (K_F), shielding (K_R) and shear stresses at the elastic-plastic interface along flanks (K_S), together with the T-stress;
- obtain values of these parameters during a constant amplitude and an overload cycle;
- observe the effect of plasticity and its influence on shielding the crack tip from the full effect of the applied load.

REFERENCES

1. Elber, W. (1970) *Eng. Fract. Mech.* **2,** 37-45.
2. Christopher, C.J., James, M.N., Patterson, E.A., Tee, K.F. (2007) *Int. J. Fract.* **148,** 361-371.
3. Christopher, C.J., James, M.N., Patterson, E.A., Tee, K.F. (2008) *Eng. Fract. Mech.* **75**, 4190–4199.
4. Pappalettere, C. (1984) *Strain* **20**, 179-180.
5. Patterson, E.A., Wang, Z.F. (1991) *Strain* **27,** 49–56.
6. Siegmann, P., Diaz-Garrido, F., Patterson, E.A. (2009) *Appl. Optics*, submitted.
7. Nurse, A.D., Patterson, E.A. (1993) *Fatigue Fract. Eng. M.* **16**, 1339-1354.

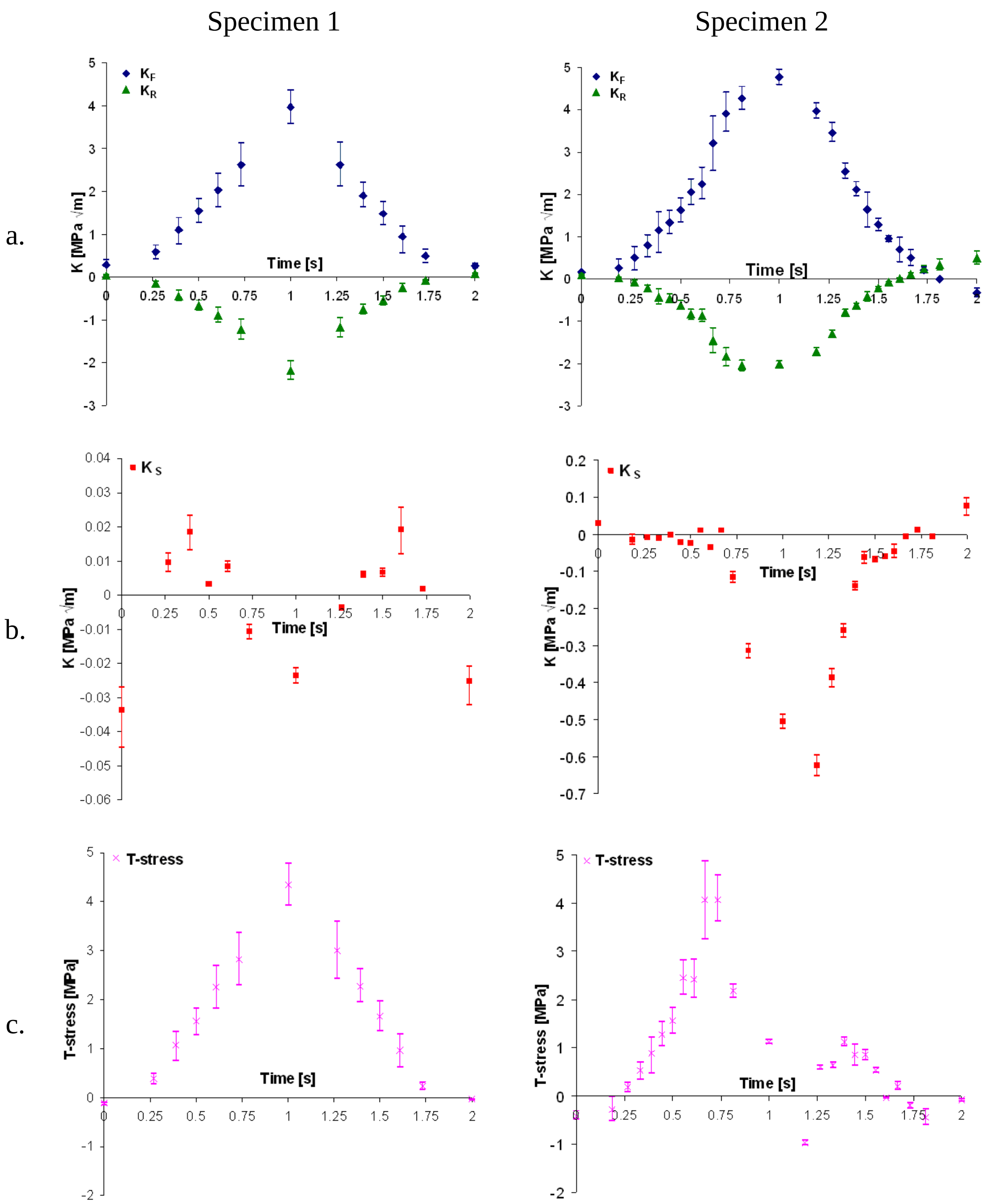

Figure 5: Trend of the evaluated parameters and confidence limits at 28.1 mm crack length for specimen 1, and at 27.9 mm during the overload cycle for specimen 2.